metals

MDPI

Article

Leaching Chalcopyrite Concentrate with Oxygen and Sulfuric Acid Using a Low-Pressure Reactor

Josué Cháidez [1,*], José Parga [2], Jesús Valenzuela [3], Raúl Carrillo [4] and Isaías Almaguer [5]

1 Metallurgical Processes, Servicios Especializados Peñoles S.A de C.V., Torreón 27300, México
2 Division of Graduate Studies and Research, Instituto Tecnológico de Saltillo, Saltillo 25280, México; jrparga@itsaltillo.edu.mx
3 Department of Chemical and Metallurgical Engineering, Universidad de Sonora, Hermosillo 83000, México; jvalen@iq.uson.mx
4 Faculty of Metallurgy, Universidad Autónoma de Coahuila, Monclova 25710, México; frrcarrillo@yahoo.com.mx
5 Metallurgical Processes, Servicios Administrativos Peñoles S.A. de C.V., Torreón 27300, México; isaias_almaguer@penoles.com.mx
* Correspondence: josue_chaidez@hotmail.com; Tel.: +52-871-121-4378

Received: 7 January 2019; Accepted: 1 February 2019; Published: 6 February 2019

Abstract: This article presents a copper leaching process from chalcopyrite concentrates using a low-pressure reactor. The experiments were carried out in a 30 L batch reactor at an oxygen pressure of 1 kg/cm^2 and solid concentration of 100 g/L. The temperature, particle size and initial acid concentration were varied based on a Taguchi L9 experimental design. The initial and final samples of the study were characterized by chemical analysis, X-ray diffraction and particle size distribution. The mass balance showed that 98% of copper was extracted from the chalcopyrite concentrate in 3 h under the following experimental conditions: 130 g/L of initial sulfuric acid concentration, temperature of 100 °C, oxygen pressure of 1 kg/cm^2, solid concentration of 100 g/L and particle size of −105 + 75 µm. The ANOVA demonstrated that temperature had the greatest influence on copper extraction. The activation energy was 61.93 kJ/mol. The best fit to a linear correlation was the chemical reaction equation that controls the kinetics for the leaching copper from chalcopyrite. The images obtained by SEM showed evidence of shrinking in the core model with the formation of a porous elemental sulfur product layer.

Keywords: Hydrometallurgical processes; Chalcopyrite; kinetics; low-pressure leaching

1. Introduction

Chalcopyrite is the most abundant sulfide copper mineral in the Earth's crust. Generally, it is associated with other compounds such as galena, sphalerite, pyrite, arsenic, antimony or bismuth sulfides; moreover, it is often bonded with valuable metals such as silver and gold.

From an environmental and economic perspective, further technological developments for obtaining high-grade copper in an efficient and cost-effective manner are desirable. Today, companies such as Beijing Nonferrous Metal, JX Nippon Mining & Metals, Freeport McMoran, Freeport Minerals, Phelps Dodge, Outotec, BHP Billiton, etc. are investing in hydrometallurgical research because of the potential associated economic benefits [1].

Specifically, hydrometallurgical processes have a series of advantages in comparison to pyrometallurgical processes, for example, the required plant capacity is smaller (<10,000 t/y of copper), there is no need for an acid plant, no dust is emitted, etc.

Hydrometallurgical pilot plant projects such as Outotec, Galvanox, Activox and AAC/UBC have implemented some of the latest technology for mineral leaching, and several demo plants have

also been installed. In particular, leaching reactors have been developed by the hydrometallurgical industry, wherein an oxidant catalyzer is commonly introduced into a pressure reactor to leach copper under varying temperatures and pressures. Table 1 lists the existing hydrometallurgical processes for leaching copper in a sulfate media, which are classified according to low, medium and high temperatures and pressures [1]. However, other aqueous media have been studied for the chalcopyrite leaching (glycine [2], nitrate [3], chloride [4], ammonium [5], etc . . .).

Most commercial plants operate under conditions of high temperature and pressure in a sulfate medium. Nevertheless, in Las Cruces (Spain), a commercial plant with an atmospheric leaching copper process has been implemented with Outotec technology [6].

The present article focuses on the leaching stage of the hydrometallurgical process to recovery copper and iron in the liquid phase using a batch reactor under low temperature and oxygen pressure conditions. In subsequent processing, lead, silver and gold may be recovered in the resulting residue by the pyrometallurgical process of lead [7–9]. The design of this technology was based on the fundaments of thermodynamics and metallurgy.

Table 1. Current hydrometallurgical processes for leaching copper. Information obtained from [1].

Leaching Processes	Name of the Processes	Country/Company	Status	Copper Mineral	Temperature (°C)	Pressure (atm)	Grinding	Acid	Oxidant Catalizer	Production (t/year)
Sulfate Medium **Low temperature and low-medium pressure**	Mount Gordon	Australia/Aditya Birla	Commercial plant	Chalcocite with pyrites	80–90	8	80%, 100 µm	Diluted H_2SO_4	O_2, ions Fe^{3+}	50,000
	Activox	Botswana (Tati)/Norilsk Process Technology	Pilot plant	Nickel-copper concentrates	90–110	10–12	Ultrafine (5–10 µm)	Diluted H_2SO_4	O_2, ions Fe^{3+}	12,000–16,000
	Las Cruces	Spain/First Quantum Minerals	Commercial plant	Chalcopyrite	90	Atmospheric	10–15 µm	Diluted H_2SO_4	H^+, O_2 and Fe^{3+}	72,000
	Galvanox	Canada (Vancouver)/UBC	Pilot plant	Chalcopyrite or enargite with pyrite	80	Atmospheric	75 µm	Diluted H_2SO_4	O_2 or air, pyrite or silver	–
Sulfate Medium	Anglo American Corporation/University of British Columbia (AAC/UBC)	South Africa (Johannesburg)/AAC-UBC	Pilot plant	Chalcopyrite	150	10–12	80%, 10 µm	Diluted H_2SO_4	O_2, surfactants (grinding required)	–
Medium temperature and low-medium pressure	Freeport McMoRan	USA (Arizona)/ Freeport McMoRan	Commercial plant	Copper sulphides concentrates	160	13.6	98%, 15 µm	Diluted H_2SO_4	Surfactants and O_2	65,200
Sulfate Medium	Freeport McMoRan	USA (Arizona)/Freeport McMoRan	Semi-commercial plant (now closed)	Chalcopyrite and molybdenite	225	32.5	Fine grinding	Diluted H_2SO_4	O_2	16,000
High temperature and high Pressure	Sepon Copper	Sepon/MMG	Commercial plant	Chalcocite and clays	80	1	100 µm	Diluted H_2SO_4	Sulfuric acid, Fe^{3+} ions	90,000
				Pyrite	230	30–32	80%, 50 µm	Diluted H_2SO_4	O_2	
Bioleaching	BioCop	Chile (Chuquicamata)/Alliance copper (BHP Billiton y CODELCO)	Commercial plant	Chalcopyrite and enargite	70–80	Atmospheric	37 µm	Diluted H_2SO_4	O_2, thermophile extreme bacteria, Fe^{3+} ions	20,000
	BacTech-Mintek	México/Peñoles	Demo plant	Chalcopyrite and copper sulphides	35–50	Atmospheric	10–20 µm	Diluted H_2SO_4	Air, moderate thermophile bacteria ions Fe^{3+}	160

2. Materials and Methods

2.1. Material and Equipment

The experiments were carried out in a stainless steel 316 L closed reactor having a volume of 30 liters and being equipped with an agitation system with 4 baffles, a security valve calibrated at 2 kg/cm^2, a rupture disc calibrated at 3 kg/cm^2, a pressure transmitter with a chemical seal and a resistance temperature detector (RTD) connected to a data logger. Also, the reactor had a controlled cooling-heating jacket. Figure 1 shows an image of the reactor.

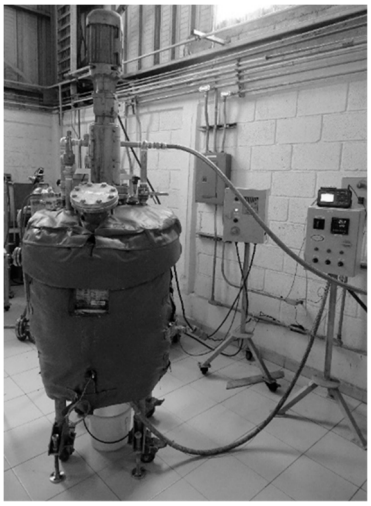

Figure 1. Batch reactor for leaching chalcopyrite concentrate.

The chalcopyrite concentrate was supplied by Peñoles (Mexico). Samples of the concentrate were characterized by X-ray diffraction (XRD, Panalytical, Empyrean model), chemical analysis (CA, PerkinElmer 8300, LECO SC230DR) and a backscattered electron (BSE) module in a scanning electron microscope (SEM, FEI, Quanta600 model) for a wider range of the mineralogical species. The chemical analysis is presented in Table 2. The carbonate content was calculated with the difference of total and organic carbon. Table 3 shows the mineralogical reconstruction via XRD and CA expressed in terms of weight percentage (Wt.%). The mineralogy species obtained by BSE-SEM are shown in Table 4 in terms of weight percentage (Wt.%).

Table 2. Chemical analysis of the chalcopyrite concentrate.

Element	Cu	Fe	As	Pb	Ca	Zn	Al	S	Si	CO_3
Wt.%	24.7	26	0.81	6.56	1.25	6.36	0.27	29.9	1.12	1.13

Table 3. Mineralogical reconstruction of the chalcopyrite concentrate.

Compounds		Weight%
Chalcopyrite	$CuFeS_2$	70.7
Galena	PbS	7.8
Sphalerite	ZnS	9.3
Gypsum	$CaSO_4$	4.1
Pyrite	FeS_2	7.8

Then, the chalcopyrite concentrate was fractionated to different sizes in a Tyler RO-TAP® Sieve Shaker using −74, −105 + 74 and −149 + 105 µm. All fractions were characterized, and no significant variation was observed in the mineralogical composition and chemical analysis. The particle size

distribution of the residues was measured in a Horiba LA 950 V2, which expressed the results in terms of the equivalent spherical diameter.

Table 4. Results of the analysis of the chalcopyrite concentrate by the SEM-BSE system.

Group	Mineral	Formula	Weight%
Sulfides	Galena	PbS	9.31
	Sphalerite	ZnS	11.09
	Chalcopyrite	$CuFeS_2$	68.65
	Tetrahedrite	$(Cu_{0.8}Fe_{0.1}Zn_{0.1})_{12}(Sb_{0.8}As_{0.2})_4S_{13}$	0.08
	Pyrite	FeS_2	2.26
	Pyrrhotite	FeS	2.00
	Arsenopyrite	FeAsS	1.27
Silver species	Native Ag	Ag	0.16
	Freibergite	$(Ag_{0.3}Cu_{0.6}Fe_{0.1})_{12}Sb_4S_{13}$	0.002
	Enargite	Cu_3AsS_4	0.01
Gangues and other oxides species	Andradite	$Ca_3Fe_2Al(SiO_4)_3$	0.41
	Apatite	$Ca_5(PO_4)_3(F, Cl, OH)$	0.004
	Augite	$(Ca,Mg,Fe)_2(Si,Al)2O_6$	0.27
	Biotite	$K(Mg, Fe)_3AlSi_3O_{10}(OH, F)_2$	0.09
	Calcite	$CaCO_3$	1.35
	Chlorite	$(Mg,Fe)_3(Si,Al)_4O_{10}(OH)_2 \cdot (Mg,Fe)_3(OH)_6$	0.10
	Quartz	SiO_2	0.48
	Diopside	$CaMgSi_2O_6$	0.23
	Grossularite	$Ca_3Al_2Si_3O_{12}$	0.36
	Moonstone	$(Ca_{0.6}Na_{0.4})Si_2AlO_8$	0.18
	Orthoclase	$K(AlSi_3O_8)$	0.48
	Ox_Fe	Fe_xO_y	0.14
	Titanite	$CaTiSiO_5$	0.02
	Others	-	1.06

2.2. Experimental Method

To clarify the effects of particle size, temperature and initial sulfuric acid concentration on copper extraction, a Taguchi 3^3 experimental design was employed. In addition, a tenth test was done using different temperatures to calculate the activation energy. The following experimental conditions were constant: residence time (7 h), oxygen pressure (1 kg/cm^2), solid concentration (100 g/L) and agitation velocity (550 RPM). Table 5 shows the experimental design.

Table 5. Taguchi L9 experimental design.

No. Test	Particle Size (μm)	Initial Acidity (g/L)	Temperature (°C)
1	−74	100	80
2	−74	130	90
3	−74	155	100
4	−105 + 74	100	90
5	−105 + 74	130	100
6	−105 + 74	155	80
7	−149 + 105	100	100
8	−149 + 105	130	80
9	−149 + 105	155	90
10	−149 + 105	130	50

The experimental procedure began with the addition of hot water (80 °C) to the reactor and the initiation of the agitation system, which was set at a low revolution speed; then, the chalcopyrite concentrate was fed into the reactor, followed by sulfuric acid. After the addition of these materials, a 2 min air purge was performed; then, the reactor was closed and pressurized to 1 kg/cm^2 with

medicinal oxygen. The agitation velocity was set at 550 RPM, and the data logger was then turned on to start recording data.

To determine the kinetics of the copper leaching process, 100 mL samples were taken from a lateral valve of the reactor at different time intervals during the test.

3. Results

3.1. Thermodynamics

The thermodynamics of copper sulfide leaching are based on the interaction of the elements required to carry out the decomposition of chalcopyrite. The main reactions that govern the leaching of copper concentrates are shown as follows:

$$CuFeS_2 + 2.5O_2 + H_2SO_4 = CuSO_4 + FeSO_4 + H_2O + S^\circ \quad (1)$$

$$CuFeS_2 + 2Fe_2(SO_4)_3 = CuSO_4 + 5FeSO_4 + 2S^\circ \quad (2)$$

$$4FeSO_4 + O_2 + 2H_2SO_4 = 2Fe_2(SO_4)_3 + 2H_2O \quad (3)$$

The Pourbaix diagrams in Figure 2 show that a low pH is required to keep copper and iron in sulfate solution. In addition, to ensure that ferric ions are present in the solution, the oxide potential must be above 0.57 V (SHE). This step enables indirect leaching via reaction 2, wherein the oxidation-reduction cycle of iron facilitates the decomposition of chalcopyrite. The Pourbaix diagrams were calculated with the software HSC 8.0.6 at 95 °C, [Cu] = 0.787 mol/L, [Fe] = 0.895 mol/L and [S] = 1 mol/L [10].

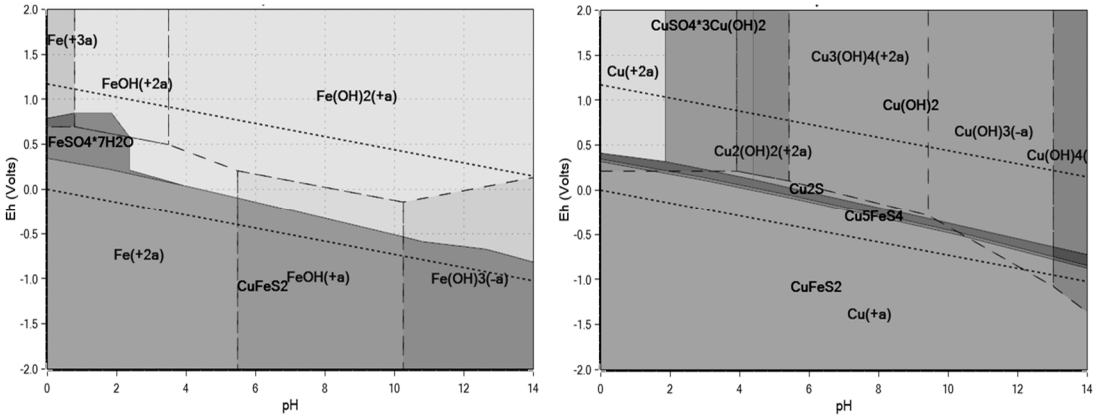

Figure 2. Cu-Fe-S Pourbaix diagrams.

3.2. Extraction and Chemical Analysis

The results of the experiment show that the main influential variables in the leaching process were temperature and initial sulfuric acid concentration. Particle size did not significantly affect the process. The results of copper extraction versus time are presented in Figure 3.

The test number 5 presented the best results according to the mass balance. Under the corresponding conditions, 97.99% of copper was extracted in 3 h of reaction. The solid shrink was 61.8% (Wt.%), and the oxygen consumption was 0.662 g O_2/g Cu fed. The density of the final solution was 1.15 g/mL, and a final oxidation-reduction potential (ORP) of 0.483V was measured in the suspension with a calomel electrode (Hg/Hg_2Cl_2).

Notably, different authors have reported percentages of copper extraction from chalcopyrite of 70% [11], 65% [12], 60% [13], 83% [14] and up to 95% [15]; in addition to 95% via the arbiter process, 98% via the Freeport McMoran method, 97–98% via the Activox process, 98% via the Albion process and 95% via the Galvanox process [1].

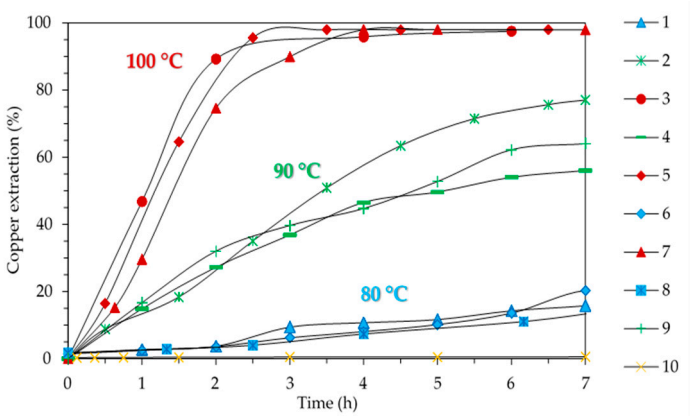

Figure 3. Copper extraction versus leaching time.

The test 5 was carried out at 100 °C with an initial sulfuric acid concentration of 130 g/L; this concentration of sulfuric acid was sufficient for reaction with species and to keep the iron in solution. Table 6 presents the CA of the residues and the solution along with the percentages of elemental distribution in the liquid phase that were obtained from the mass balance.

Table 6. Chemical analysis of the test 5 residue (Wt.%), chemical analysis of the solution (g/L) and the elemental distribution in the liquid phase (%) of the leaching process.

Element	Residue (Wt.%)	Solution (g/L)	Distribution in Liquid Phase (%)
Cu	1.12	22.83	97.99
Fe	3.65	27.26	94.69
As	0.08	0.8	95.9
Pb	13.2	0.055	1.0
Zn	0.25	5.96	98.24
S°	56.2	0.0	0.0
Fe^{2+}	-	3.89	-
H_2SO_4	-	45.45	-

The leaching solution contained a high percentage of zinc, copper and iron because of the solubility of these elements in the utilized sulfate medium (given the temperature and acid concentration). In a global process view, it is important to consider that the solution could be treated in a solvent extraction and electrowinning stages for the production of electrolytic copper. The raffinate from solvent extraction could be neutralized with calcium carbonate to precipitate ferric ions, zinc, arsenic and minor elements; then, the solution could be recycled to the direct leaching stage.

The iron in the residue mainly corresponded with pyrite, which requires higher temperature and pressure for decomposition. Table 7 shows the species present in the solid phase in terms of weight percentages, including elemental sulfur (64.1%), anglesite (19.3%), silica (5%), pyrite (5.7%), unreacted chalcopyrite (3.23%) and gypsum (2.3%).

Table 7. Mineralogical reconstruction of the leaching residue in test 5.

Compounds		Wt.%
Chalcopyrite	$CuFeS_2$	3.23
Anglesite	$PbSO_4$	19.3
Gypsum	$CaSO_4$	2.3
Silica	SiO_2	5.0
Pyrite	FeS_2	5.7
Elemental sulfur	S_8	64.1

From an economic perspective, the recovery of valuable minerals in residues following the hydrometallurgical treatment of chalcopyrite concentrates is important. The high content of elemental sulfur could reduce the profitability of recovering valuable metals by cyanidation or melting processes.

Table 8 presents the final particle size distribution of the P5 test. As expected, the particle size decreased considerably from 100% +74 µm to 90% −16.92 µm because of the leaching of chalcopyrite particles and the formation of elemental sulfur.

Table 8. Particle size distribution of the resulting residue from chalcopyrite leaching in test P5.

Particle Size Distribution		
D90%	D50%	D10%
16.92	11.00	6.99

Figure 4 shows electron images obtained by SEM-BSE of unreacted chalcopyrite and galena particles, which were identified by SEM-EDS. The porous layer of elemental sulfur surrounding the particles can be observed. These particles are indicative of the shrinking core model, wherein a layer of elemental sulfur is formed as a product. However, the high extraction percentage of copper obtained in a short time (3 h) indicates that the elemental sulfur layer does not passivate the leaching of the chalcopyrite concentrate.

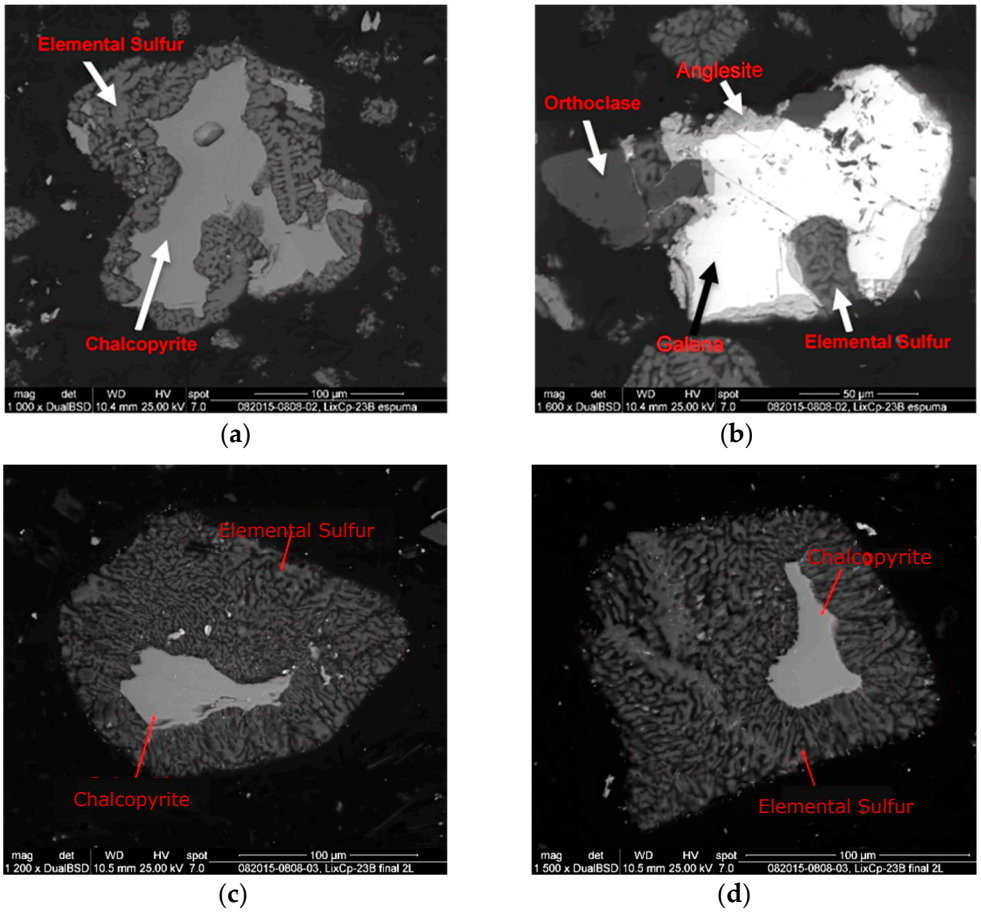

Figure 4. Punctual microanalysis by SEM-BSE-EDS in the leached residue of test P5. (**a**) Unreacted chalcopyrite particle, (**b**) unreacted galena particle, (**c**) unreacted Chalcopyrite particle, (**d**) unreacted Chalcopyrite particle.

Figure 5 shows the microstructure and the X-ray mapping by SEM-EDS for sulfur, copper and iron of the unreacted chalcopyrite particle.

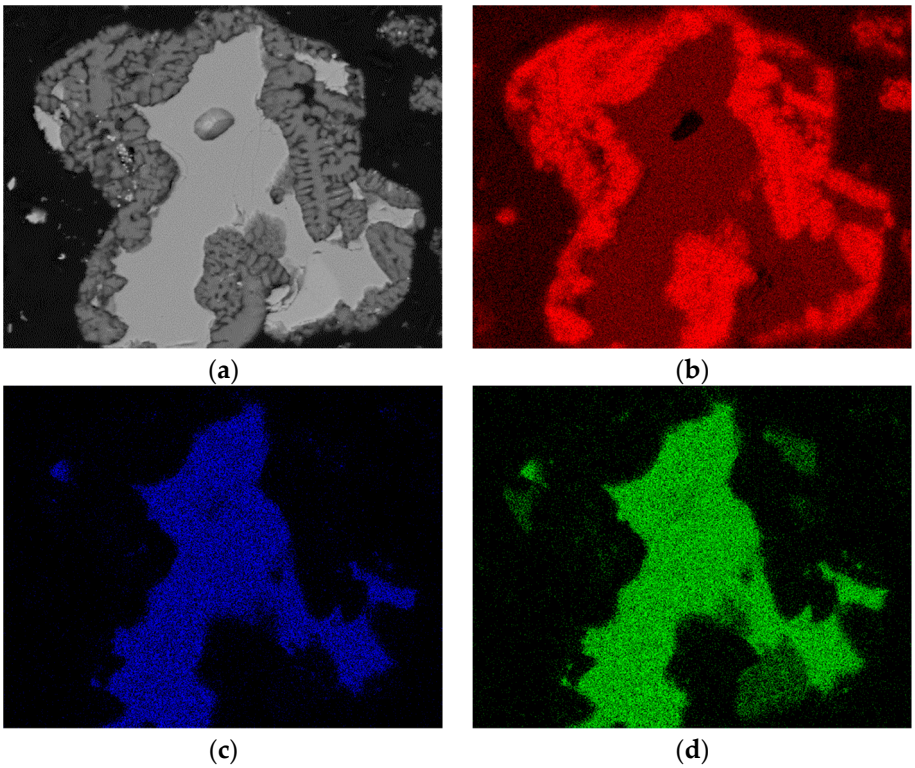

Figure 5. X-ray mapping by SEM-EDS in the unreacted chalcopyrite particle of test P5. (**a**) electron image, (**b**) S, (**c**) Cu, (**d**) Fe.

In Figure 6, the temperature profile, in addition to the partial and accumulated oxygen consumption, are shown. At 2 h, oxygen consumption reaches its maximum and then decreases after this point.

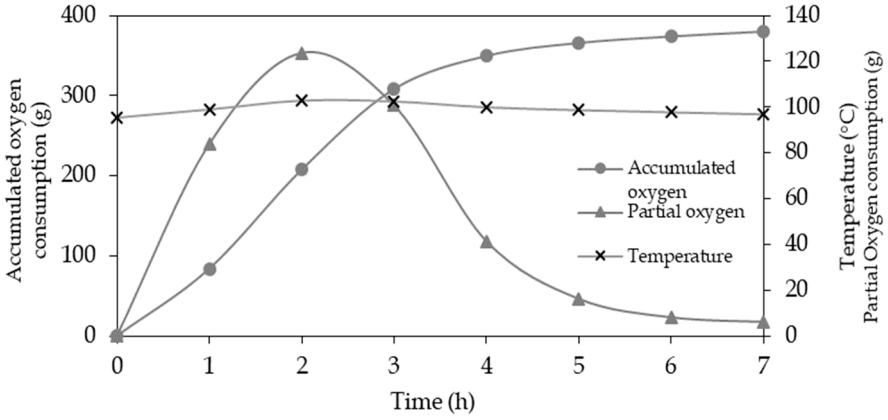

Figure 6. Temperature and partial and accumulative oxygen consumption over time in test P5.

A similar finding was observed for the iron concentration in solution; ferrous ions reached their maximum concentration at 2 h and then decreased. This could explain the chalcopyrite leaching as a two steps process.

Specifically, the first step occurred within the initial 2 h of the test, wherein most of the chalcopyrite was decomposed at temperatures above 95 °C. The second step occurred when the remaining ferrous ions were oxidized to ferric iron. Depending on the next stages, which are related with the liquid phase (iron purification or solvent extraction), the Fe^{3+}/Fe^{2+} relation must be as high as possible to

ensure that the process is not affected. In Figure 7, the concentration profile of iron and ferrous ions during leaching is shown.

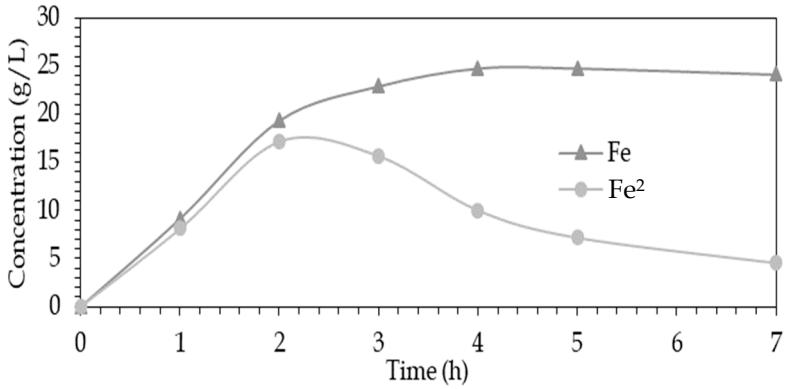

Figure 7. Concentration of iron and ferrous ions over time in test P5.

3.3. Statistical Analysis

As mentioned in Table 5, this study is based on a modified Taguchi L9 experimental design with three levels for three independent variables or parameters. An additional experiment was realized (Test 10): analysis of variance (ANOVA) of the experimental tests data at different conditions was used to evaluate the effect of each individual variable. The results of Test 10 were not included in ANOVA due the difference of temperature between the lowest and the average and the small amount of Cu extraction observed.

Table 9 shows the effects of each parameter using the ANOVA module of the Minitab 15 software. The table shows the values of degree freedom (DF), sum of squares (SS), media of squares (MS), Fisher ratio (F), probability level (Prob Level) and the probability that a false null hypothesis can be rejected (Power) with a 95% confidence level ($\alpha = 0.05$). According to F, Prob Level and Power values, ANOVA shows that under the studied conditions, temperature is the most important factor for copper extraction and oxygen consumption. The results also indicated that within the analyzed range, the other two variables studied (initial acid and particle size) did not have a statistically-significant effect.

Table 9. Analysis of variance (ANOVA) for Cu extraction.

Parameter	DF	SS	MS	F	Prob Level	Power
			Cu Extraction			
Temperature	2	10160.97	5080.487	98.26	0.010075 *	0.993017
Initial acid	2	114.2358	57.11791	1.1	0.47513	0.10105
Particle size	2	36.89769	18.44884	0.36	0.737023	0.066798
S	2	103.4102	51.70508			
Total (Adjusted)	8	10415.52				
Total	9					
			Oxygen Consumption			
Temperature	2	0.2263376	0.1131688	46.99	0.020836 *	0.909376
Initial acid	2	4.52×10^4	2.26×10^4	0.09	0.91428	0.054443
Particle size	2	1.85×10^3	9.25×10^4	0.38	0.722385	0.06808
S	2	4.82×10^3	2.41×10^3			
Total (Adjusted)	8	0.2334562				
Total	9					

* $\alpha = 0.05$.

Figure 8 shows the correlations of temperature, initial acid concentration and particle size with percentage of copper extraction. As observed, temperature had the greatest effect on the process of leaching copper from chalcopyrite concentrates. Figure 9 shows the correlations of temperature, initial acid concentration and particle size with oxygen consumption. As expected, temperature

once again had the greatest effect on oxygen consumption, whereas particle size and initial acid concentration had no clear influence.

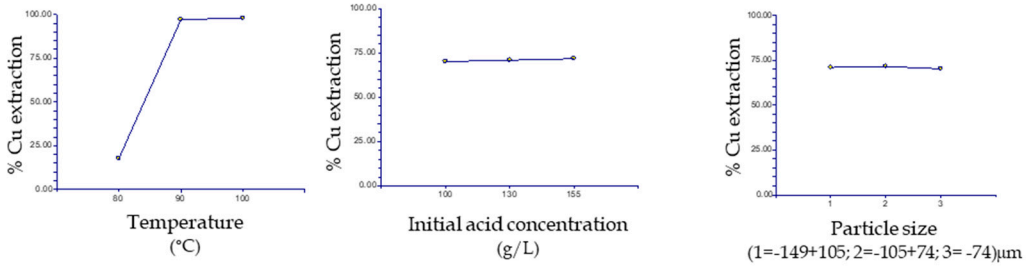

Figure 8. Correlations of temperature, initial acid concentration and particle size with extraction of copper.

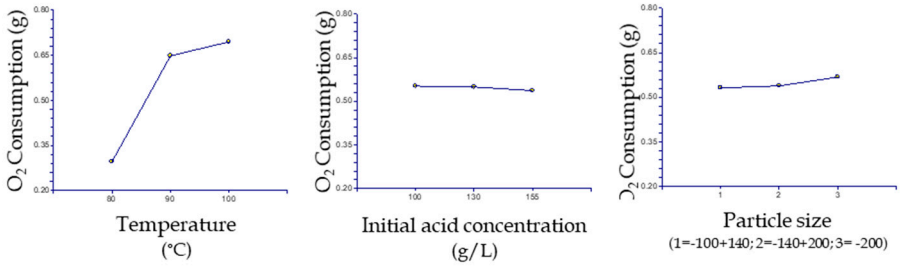

Figure 9. Correlations of temperature, initial acid concentration and particle size with oxygen consumption.

According to the above results the copper extraction can be calculated with the following multiple regression equation:

$$\text{Copper extraction (\%)} = -146.382 + 2.253\ \text{T} + 0.0957\ \text{Acid} - 0.0554\ \text{Size} \quad (4)$$

where T is the temperature expressed in °C; Acid is the initial acid concentration in g/L and size is the particle size of the chalcopyrite concentrate in µm.

3.4. Effect of Temperature

As observed in Figure 3, the different tests can be categorized into three groups with differing rates of reaction that were principally determined by temperature. The tests of the first group were carried out at 100 °C (tests 3, 5 and 7) and resulted in 97% copper extraction within 3 h. The second group (tests 2, 4 and 9) resulted in 55–77% copper extraction within 7 h. The tests of the final group were carried out at 80 °C (tests 1, 6 and 8) and resulted in 10–20% copper extraction within 7 h.

To highlight the required temperature for activating the decomposition of chalcopyrite concentrates, test 5 was replicated with a slowly-increasing temperature. Figure 10 shows the percentage of copper extraction and temperature versus time. As observed, the temperature had to reach 92–95 °C to decompose the chalcopyrite in the concentrate.

3.5. Effect of Particle Size

In the three groups that formed with respect to different reaction temperatures (Figure 3), the reactions were also faster for concentrates of small particle size; nevertheless, in the group that reacted at 100 °C, the −149 + 105 µm chalcopyrite concentrate reacted more rapidly than the concentrate filtered by −75 µm. The reactions in this group could have been slowed by the heat transfer from the jacket of the reactor to the suspension, resulting in different rates of reaction.

Thus, even when the chalcopyrite concentrate was a larger particle size (−149 + 105 µm), the copper extraction was not affected at 100 °C, and a similar level of extraction of copper was obtained.

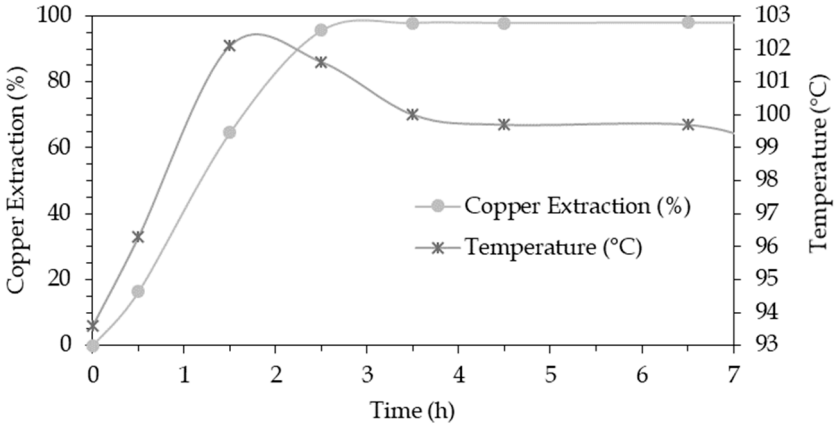

Figure 10. Copper extraction and temperature for the test 5 replicated.

3.6. Effect of Acidity

The initial sulfuric acid concentration in the suspension must be calculated based on the stoichiometry of the compounds that consume acid and the final acid concentration required to keep iron and copper in solution.

According to Figure 8, the initial sulfuric acid concentration is not significant for copper extraction. But in other exploratory tests carried out with the same copper concentrates at 100 °C under the same conditions, the suspension was found to require at least 15 g/L of sulfuric acid in solution to avoid the precipitation of iron as plumbojarosite in the residue. Thus, to prevent any problems in the recovery of valuable metals resulting from the presence of elemental sulfur and plumbojarosite in residues, and to avoid any potential impact on the profitability of operations, the initial sulfuric acid concentration is important to consider.

$$3Fe_2(SO_4)_3 + 12H_2O + PbSO_4 = 2Pb_{0.5}Fe_3(SO_4)_2(OH)_6 + 6H_2SO_4 \quad (5)$$

Figure 11 shows the iron and acid concentrations in solution, the percentage of plumbojarosite in the residue and the percentage of copper extraction versus time in an exploratory test. The initial acid concentration was 72 g/L, yet it diminished to 10–15 g/L. At 15 g/L of sulfuric acid in solution, the precipitation of plumbojarosite in the residue began, leading to a clear decrease in the iron in solution from 23.6 g/L to 15.8 g/L.

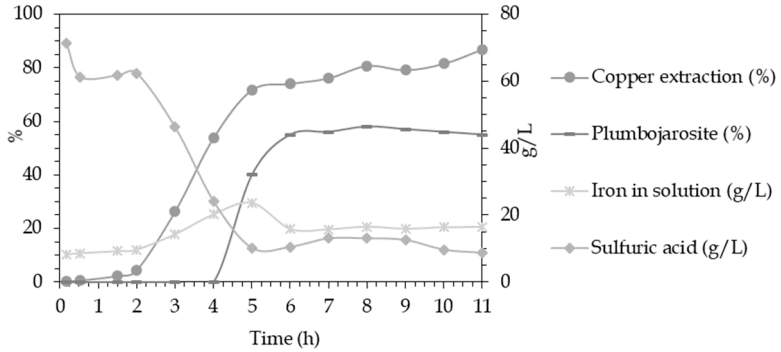

Figure 11. Results of an exploratory test with a low acid concentration in the reaction solution.

A comparison of the copper extractions with low and high acid concentrations in the reaction solution shows that passivation was promoted by a lack of acid in the solution, which, in turn, produced a plumbojarosite layer on the chalcopyrite surface (see Figure 12).

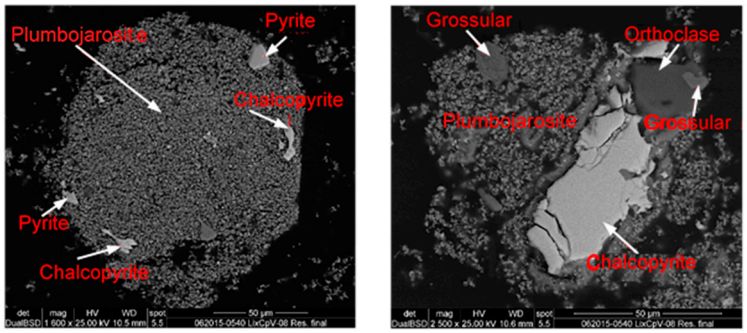

Figure 12. Precipitation of plumbojarosite under low acidity conditions during leaching. (**a**) Plumbojarosite particle, (**b**) unreacted chalcopyrite particle.

The mass balance demonstrated that the ratio of sulfuric acid consumed (real) to that calculated by stoichiometry is given by Equation (6).

$$1.25 = \frac{\text{gReal}}{\text{g Stoichiometric} + \text{gtoreach}\ [\text{finalacid}] = 45\ \text{g/L}} \quad (6)$$

3.7. Kinetics

To determine the kinetics of the leaching process described herein, the shrinking core (product layer) model was applied to the real batch process considering the scanning electron microscopy (SEM) images of partly-reacted particles (Figure 4). The controlling step of the reaction was based on a comparison of the experimental data and assessment of which controlling model gives the best fit to the data. If the chemical reaction mechanism is assumed to be the controlling step, $1 - (1 - X)^{1/3}$ (X = conversion) is plotted as a function of time for the experimental data, and if the plot gives a linear correlation, the assumption is considered to be correct. Analogously, $1 - 3(1 - X)^{2/3} + 2(1 - X)$ (diffusion as controlling mechanism) can be plotted for the data when a non-porous product layer is formed [16,17].

The results show that the chemical reaction is the controlling stage for leaching copper from chalcopyrite concentrate. Figure 13 shows the linear regressions of the 9 tests. The equation of the chemical reaction as the controlling step is also shown as follows (Equation (7)).

$$kt = 1 - (1-X)^{(1/3)} \quad (7)$$

where t is time and k is the apparent velocity constant.

Table 10 shows the apparent velocity constants (k) and the determination coefficient (R^2) of the linear regression of the chemical reaction model for all 10 tests.

Table 10. Results for the linear regression of the chemical reaction model of all 10 tests.

Test	P1	P2	P3	P4	P5	P6	P7	P8	P9	P10
Slope (k)	0.006	0.032	0.12	0.031	0.096	0.009	0.112	0.01	0.035	0.0001
R^2	0.973	0.81	0.938	0.97	0.806	0.929	0.919	0.973	0.968	0.835

To calculate the activation energy, logarithms were applied to the Arrhenius equation (Equation (8)) to reformulate it as a linear equation. Accordingly, the logarithm of the apparent velocity constants versus the inverse of temperature of tests P3, P8, P9 and P10 is shown in Figure 14.

$$\text{Log}k = \text{LogA} - \log\,(\text{E/R})^{\,(1/\text{T})} \quad (8)$$

An activation energy of 61.93 kJ/mol was determined from the slope of the straight line in Figure 14. According to Habashi (1999), a chemically-controlled process is usually greater than 41.8 kJ/mol [18].

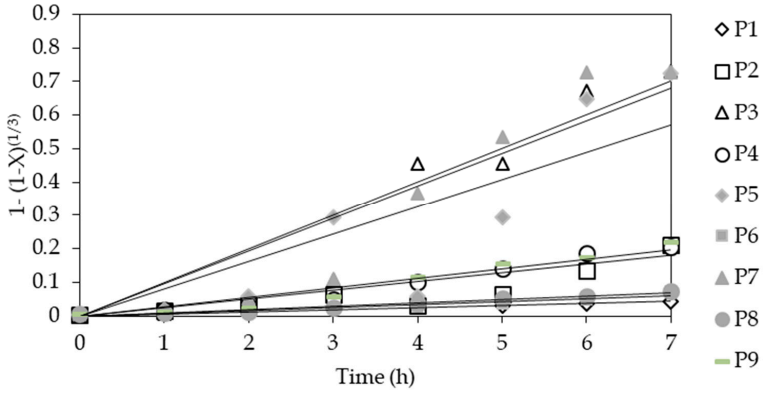

Figure 13. Linear regression of the chemical reaction model.

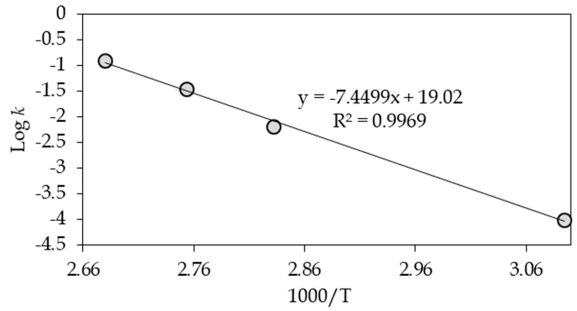

Figure 14. Logarithm of the apparent velocity constant versus the inverse of temperature.

In order to compare the activation energy with similar processes, Table 11 shows the results reported by some authors in literature. It can be observed that the activation energy for processes that use sulfuric acid, ferric ions and/or oxygen is similar to the obtained in this work that use sulfuric acid and oxygen. In the work reported by Padilla et al. (2008), they use also only sulfuric acid and oxygen in a pressure reactor and a copper extraction of 95% was obtained at an oxygen pressure of 5 kg/cm^2, 125 °C in 4 h [19]. In our work, we obtained 98% Cu extraction under less extreme conditions: oxygen pressure of 1 kg/cm^2, 100 C and only 3 h.

Table 11. Results reported in literature of activation energy for chalcopyrite leaching.

Leach Media	Activation Energy (kJ/mol)	Reference	Temperature Range (°C)
$K_2Cr_2O_7 + H_2SO_4$	24	[11]	50–97
$H_2O_2 + H_2SO_4$	39	[13]	30–80
$O_2 + H_2SO_4$	93.5	[19]	125–140
H_2SO_4	42.4	[20]	160–180
$K_2Cr_2O_7 + H_2SO_4$	48–54	[21]	-
$Fe_2(SO_4)_3 + H_2SO_4$	79.5	[22]	50–90
$H_2O_2 + H_2SO_4$	30	[23]	-
$Fe_2(SO_4)_3 + H_2SO_4$	21 ± 5	[24]	55–85
$NaNO_3 + H_2SO_4$	83	[25]	70–90
$Fe_2(SO_4)_3 + Cu^{2+} + NaCl + H_2SO_4$	66.6	[26]	70–90
$NaNO_2 + H_2SO_4$	34.0	[27]	80–120
$H_2SO_4 + O_2$	61.93	Present work	80–100

Padilla et al. (2008) required a higher activation energy than the present work; this is due to the design of reactor used. The reactor used in the present work promotes a high interaction between the

solid-gas-liquid phases, improving the mass transport at the gas-solid interface. Thus, the activation energy required for the leaching of chalcopyrite decreases.

4. Conclusions

In the present study, the copper leaching of chalcopyrite concentrate in a 30-L batch reactor was described. The experimental results showed that it is possible to extract 98% of copper in only 3 h. This result indicates a fast process compared with others reported in literature.

The best result (98% in 3 h) was obtained under the following reaction conditions: 130 g/L of initial sulfuric acid concentration, temperature of 100 °C, oxygen pressure of 1 kg/cm^2, solid concentration of 100 g/L and concentrate particle size of $-104 + 75$ μm.

The copper leaching is controlled chemically. Then, the elemental sulfur layer exposed on the unreacted particles of chalcopyrite does not interfere with the mass transport or the interactions between phases.

A statistical analysis showed that temperature is the most important variable influencing the extraction of copper and oxygen consumption. A temperature of at least 92 °C (61.93 kJ/mol) is necessary to activate the decomposition of chalcopyrite.

The initial sulfuric acid concentration must also be considered as an important variable from an economic perspective. An excess of sulfuric acid will increase the neutralizing agent in the posterior stages of the leaching process, whereas a lack of sulfuric acid could result in the precipitation of iron as plumbojarosite, and could therefore create difficulties in the recovery of valuable metals at later stages.

Author Contributions: Conceptualization, J.C. and R.C.; Formal analysis, J.C.; Investigation, J.C., J.P., J.V. and R.C.; Methodology, J.C., J.V. and R.C.; Project administration, I.A.; Resources, J.P. and I.A.; Supervision, J.P., R.C. and I.A.; Validation, J.C. and I.A.; Writing—original draft, J.C.; Writing—review & editing, J.V. and R.C.

Acknowledgments: The authors gratefully acknowledge the technical support of the National Institute of Technology of México and Servicios Especializados Peñoles S.A. de C.V. for the financial support.

Conflicts of Interest: The authors declare no conflict of interest.

References

1. Taylor, A. *A-Z of Copper Ore Leaching Short Course Manual*; ALTA Metallurgical Services: Perth, Australia, 2014.
2. Eksteen, J.; Oraby, E.; Tanda, B. An alkaline glycine-based process for copper recovery and iron rejection from chalcopyrite. In Proceedings of the IMPC 2016—28th International Mineral Processing Congress, Québec City, QC, Canada, 11–15 September 2016; ISBN 9781926872292.
3. Hernández, P.; Taboada, M.; Herreros, O.; Graber, T.; Ghorbani, Y. Leaching of Chalcopyrite in Acidified Nitrate Using Seawater-Based Media. *Minerals* **2018**, *8*, 238. [CrossRef]
4. Watling, H. Chalcopyrite hydrometallurgy at atmospheric pressure: 2. Review of acidic chloride process options. *Hydrometallurgy* **2014**, *146*, 96–110. [CrossRef]
5. Turan, M.; Arslanoglu, H.; Altundogan, H. Optimization of the leaching conditions of chalcopyrite concentrate using ammonium persulfate in an autoclave system. *J. Taiwan Inst. Chem. Eng.* **2015**, *50*, 49–55. [CrossRef]
6. Frias, C.; Vera, E.; Romero, A.; Blanco, J. Flotation and hydroprocessing of bulk concentrate from Las Cruces Mine. In Proceedings of the Pb-Zn Conference, Düsseldorf, Germany, 14–17 June 2015.
7. Chen, S.; Berg, C.; Mansikkaviita, H.; Dezi, W.; Rong, Z. Drying Blended Concentrates by Kumera Steam Dryer for Kivcet Lead Flash Smelting. In Proceedings of the Pb-Zn Conference, Düsseldorf, Germany, 14–17 June 2015; pp. 257–265.
8. Burrows, A.; Azekenov, T.; Zatayev, R. Lead ISASMELTTM Operation at Ust-Kamenogorsk. In Proceedings of the Pb-Zn Conference, Düsseldorf, Germany, 14–17 June 2015; pp. 245–256.
9. Wang, C.; Yin, F.; Gao, W.; Ma, B. The research and Engineering Practice of the Lead Oxygen-Enrichment Flash Smelting. In Proceedings of the Pb-Zn Conference, Düsseldorf, Germany, 14–17 June 2015; pp. 273–284.
10. Outotec. *Software HSC Chemestry 8*; Continuous Research and Development: Pori, Finland, 2014.

11. Aydogan, S.; Ucar, G.; Canbazoglu, M. Dissolution kinetics of chalcopyrite in acidic potassium dichromate solution. *Hydrometallurgy* **2006**, *81*, 45–51. [CrossRef]
12. Xian, Y.; Wen, S.; Deng, J.; Liu, J.; Nie, Q. Leaching chalcopyrite with sodium chlorate in hydrochloric acid solution. *Can. Metall. Q.* **2012**, *51*, 133–140. [CrossRef]
13. Adebayo, A.; Ipinmoroti, K.; Ajayi, O. Dissolution kinetics of chalcopyrite with hydrogen peroxide in sulphuric acid medium. *Chem. Biochem. Eng. Q.* **2003**, *17*, 213–218.
14. Aleksei, K.; Kirill, K.; Stanislav, N. Pressure Leaching of Chalcopyrite Concentrate. *AIP Conf. Proc.* **2018**. [CrossRef]
15. O'brien, R.; Macdonald, C.; Meadows, N. *Chloride–Sulphate Leaching from Chalcopyrite Ores from Sabah. ALTA Copper Sulphides Symposium and Copper Hydrometallurgy Forum (GoldCoast, QLD)*; ALTA Metallurgical Services: Melbourne, Australia, 1999.
16. Levenspiel, O. *Chemical Reaction Engineering*, 3rd ed.; Wiley: New York, NY, USA, 1999; ISBN 9780471254249.
17. Grénman, H.; Salmi, T.; Murzin, D.Y. Solid-liquid reaction kinetics—Experimental aspects and model development. *Rev. Chem. Eng.* **2011**, *27*, 53–77. [CrossRef]
18. Habashi, F. *Kinetics of Metallurgical Process*; Métallurgie Extractive: Québec City, QC, Canada, 1999; ISBN 978-2-922686-60-9.
19. Padilla, R.; Pavez, P.; Ruiz, M. Kinetics of copper dissolution from sulfidized chalcopyrite at high pressures in H_2SO_4–O_2. *Hydrometallurgy* **2008**, *91*, 113–120. [CrossRef]
20. Baisui, H.; Batnasan, A.; Kazutoshi, H.; Yasushi, T.; Atsushi, S. Leaching and Kinetic Study on Pressure Oxidation of Chalcopyrite in H_2SO_4 Solution and the Effect of Pyrite on Chalcopyrite Leaching. *J. Sustain. Metall.* **2017**, *3*, 528–542. [CrossRef]
21. Antonijevic, M.; Jankovic, Z.; Dimitrijevic, M. Investigation of the kinetics of chalcopyrite oxidation by potassium dichromate. *Hydrometallurgy* **1994**, *35*, 187–201. [CrossRef]
22. Al-Harahsheh, M.; Kingman, S.; Hankins, N.; Somerfield, C.; Bradshaw, S.; Louw, W. The influence of microwaves on the leaching kinetics of chalcopyrite. *Miner. Eng.* **2005**, *18*, 1259–1268. [CrossRef]
23. Mahajan, V.; Misra, M.; Zhong, K.; Fuerstenau, M. Enhanced leaching of copper from chalcopyrite in hydrogen peroxide-glycol system. *Miner. Eng.* **2007**, *20*, 670–674. [CrossRef]
24. Kaplun, K.; Li, J.; Kawashima, N.; Gerson, A. Cu and Fe chalcopyrite leach activation energies and the effect of added Fe^{3+}. *Geochim. Cosmochim. Acta* **2011**, *75*, 5865–5878. [CrossRef]
25. Sokic, M.; Markovic, B.; Zivkovic, D. Kinetics of chalcopyrite leaching by sodium nitrate in sulphuric acid. *Hydrometallurgy* **2009**, *95*, 273–279. [CrossRef]
26. Veloso, T.; Peixoto, J.; Pereira, M.; Leao, V. Kinetics of chalcopyrite leaching in either ferric sulphate or cupric sulphate media in presence of NaCl. *Int. J. Miner. Process.* **2016**, *148*, 147–154. [CrossRef]
27. Gok, O.; Anderson, C.; Cicekli, G.; Cocen, E. Leaching kinetics of copper from chalcopyrite concentrate in nitrous-sulfuric acid. *Physicochem. Probl. Miner. Process.* **2013**, *50*, 339–413. [CrossRef]